Laser synthesizing NiAl intermetallic and TiC reinforced NiAl intermetallic matrix composite

Minlin Zhong, Xiangyang Xu, Wenjin Liu, and Hongqing Sun

Citation: Journal of Laser Applications **16**, 160 (2004); doi: 10.2351/1.1771106
View online: http://dx.doi.org/10.2351/1.1771106
View Table of Contents: http://scitation.aip.org/content/lia/journal/jla/16/3?ver=pdfcov
Published by the Laser Institute of America

Laser synthesizing NiAl intermetallic and TiC reinforced NiAl intermetallic matrix composite

Minlin Zhong[a)]
Laser Processing and Rapid Prototyping Research Center, Department of Mechanical Engineering, Tsinghua University, Beijing, 100084, China

Xiangyang Xu
Laboratory for Surface Modification, Institute of Mechanics, Chinese Academy of Sciences, Beijing 100080, China

Wenjin Liu and Hongqing Sun
Laser Processing and Rapid Prototyping Research Center, Department of Mechanical Engineering, Tsinghua University, Beijing, 100084, China

(Received 16 November 2002; accepted for publication 6 February 2004)

The NiAl intermetallic layers and NiAl matrix composite layers with TiC particulate reinforcement were successfully synthesized by laser cladding with coaxial powder feeding of Ni/Al clad powder and Ni/Al+TiC powder mixture, respectively. With optimized processing parameters and powder mixture compositions, the synthesized layers were free of cracks and metallurgical bond with the substrate. The microstructure of the laser-synthesized layers was composed of β-NiAl phase and a few γ phases for NiAl intermetallic; unmelted TiC, dispersive fine precipitated TiC particles and refined β-NiAl phase matrix for TiC reinforced NiAl intermetallic composite. The average microhardness was 355 $HV_{0.1}$ and 538 $HV_{0.1}$, respectively. Laser synthesizing and direct metal depositing offer promising approaches for producing NiAl intermetallic and TiC-reinforced NiAl metal matrix composite coatings and for fabricating NiAl intermetallic bulk structure. © *2004 Laser Institute of America.*

Key words: laser synthesizing, NiAl intermetallic, NiAl matrix composite, particulate reinforcement

I. INTRODUCTION

NiAl intermetallic is considered a potential high temperature structural material for astronautics and aeronautics due to its high melting point, low density, excellent oxidation, and hot corrosion resistance at elevated temperatures.[1–3] However, the tensile ductility and fracture toughness of intermetallic at ambient temperature are usually poor. Further, the high temperature strength is still insufficient in most cases. This directly restricts its operational temperature and deteriorates its machinability.[4–6] Therefore, NiAl intermetallic alloys have rarely been applied in practice to date.

Various strengthening and toughening approaches have been explored for improving both the high temperature strength and the ambient ductility and toughness of NiAl intermetallics.[1,2,7,8] These techniques mainly include solid-solution strengthening, precipitating strengthening, dispersive strengthening, particulate reinforcement, directional solidification, and single crystal. However, with the increase of the high temperature creep strength by some strengthening methods, the ambient temperature tensile ductility and fracture toughness of NiAl intermetallic normally decrease considerably. Thus, the principal issue is to improve both the high temperature strength of the NiAl intermetallic and its ambient temperature ductility and toughness.[7–9] Particulate reinforcement is considered an effective method of improving the strength and toughness of NiAl intermetallic.[10,11] Laser cladding offers an excellent possibility for producing hard-facing coatings, particulate reinforced metal matrix composites, as well as new alloy development and rapid manufacturing of metallic components. By means of laser cladding, it is possible to synthesize NiAl intermetallic, to improve its high temperature strength, to increase its ambient temperature ductility and toughness, and to deposit directly or even to manufacture near net shape NiAl intermetallic components.

This article presents the results of research on synthesizing NiAl intermetallic and TiC particulate reinforced NiAl intermetallic matrix composite (IMC) using laser cladding with coaxial feeding of Ni/Al clad powder or Ni/Al+TiC powder mixture, respectively.

II. EXPERIMENTAL PROCEDURES

The experiments were carried out in a laser system consisting of a PRC 3000 3 kW continuous wave fast axial flow CO_2 laser. A THPF-1 powder feeder and a THCN-3 patented coaxial nozzle were used for coaxial powder delivery. The substrate material was a commercial mild steel plate with thickness of 10 mm; its surface was mechanically ground

a)Electronic mail: zhml@tsinghua.edu.cn

and carefully cleaned with gasoline and acetone before experiments. The powder material was Ni/Al clad powder (Al particles are cladded by Ni particles) with the size of $-75-+49$ μm, in stoichiometric composition of the NiAl intermetallics. Approximately 15–20 wt % of TiC powder (-200 meshes) was added to the Ni/Al powder for particulate reinforcement. The Ni/Al powder and TiC powder were mechanically mixed for 1 h, dried in a tube furnace for 2 h at 100 °C, and then slow cooled to room temperature.

The laser processing parameters were: laser power $P=1.5$ kW, scanning velocity $V=4$ mm/s, laser beam diameter $D=5$ mm, and powder feeding rate $Q=4.0$ g/min. Argon was used as a shielding gas for protection of the melt pool. Each specimen was overlap deposited in three layers.

The microstructures of the synthesizing layers were observed and analyzed by a CSM950 scanning electron microscope. The compositions were determined by Link ISIS energy dispersive spectrometry (EDS). The phases were identified with a Rigida x-ray diffractometer. The microhardness was measured using a Vicker hardness tester at 100 g loads.

III. EXPERIMENTAL RESULTS AND DISCUSSIONS

A. Laser synthesizing NiAl intermetallics

Experimental results (Fig. 1) demonstrated that laser synthesizing NiAl intermetallic by feeding of the Ni/Al clad powder may result in severe cracks in the layer depending on the processing parameters (for example: laser power from 1750 to 2000 W, beam diameter of 3 mm, scanning speed from 7.5 to 10 mm/s, and powder feed rate from 2.7 to 3.2 g/min). The cracking phenomenon was characterized in the following aspects: (1) The cracks mainly originated at the surface of the deposited layer and then propagated downward to the interior of the layer [Fig. 1(a)]; (2) Some of the cracks originated at the interface between the deposited layer and the substrate and then developed into the layer [Figs. 1(a) and 1(b)]; and (3) Most cracks propagated along the grain boundary [Fig. 1(c)]. The cracking in the laser-synthesized NiAl intermetallic was mainly attributed to the rapid heating and cooling, to the difference in the thermal expansion coefficient between the synthesized layer and the substrate, and to the brittleness of the NiAl intermetallic itself.

However, dense synthesized layers free of cracks and porosities were achieved [Fig. 2(a)] under optimized processing parameters: laser power of 1.5 kW; beam diameter of 5 mm; scanning speed of 4 mm/s; and powder feed rate of 4.2 g/min. The deposited layer was 3.37 mm in width and 0.96 mm in height. EDS analysis indicated that the deposited layer contains about 49 at. % of Ni, 40 at. % of Al, and 11 at. % of Fe (the possible C from the melted substrate is not detected in this analysis). About 11 at. % of Fe was in the layer due to the dilution of the substrate. The atom ratio of Ni and Al in the synthesized layer was about 1.2:1 though the original powder mixture was made according to the stoichiometric composition of NiAl intermetallic which is 1:1. This means that some Al was lost due to evaporation during the laser cladding process and the composition was dramatically changed.

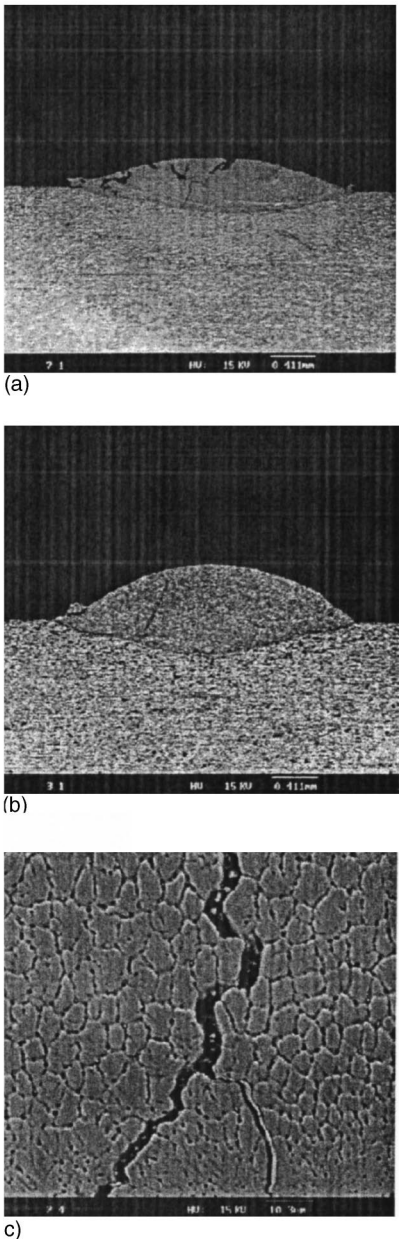

FIG. 1. Cracking phenomena in laser synthesized NiAl intermetallic layers: (a) cracks originated at the surface, (b) cracks originated at the interface, and (c) cracks propagated along the grain boundary.

The relationship between the dilution rate and the processing parameters is illustrated in Fig. 3. The dilution rate is defined as the Fe atomic percentage in the composition of the synthesized layer. Figure 3 indicates that an increase of the laser power dramatically increases the dilution of the synthesized layer, while a change in the scanning speed has less effect on the dilution. There is an optimized powder feed rate for less dilution. The powder feed rate can not be either too large or too small for a less dilution layer.

Figure 4 identifies the relationship between the Al atomic percentage within the synthesized layer and the processing parameters. Increasing the laser power slightly decreases the Al content in the layer, which increases the Al lost during the cladding process. Increasing the scanning speed and the powder feed rate slightly increases the Al con-

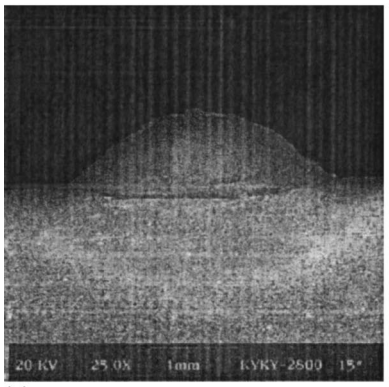

(a)

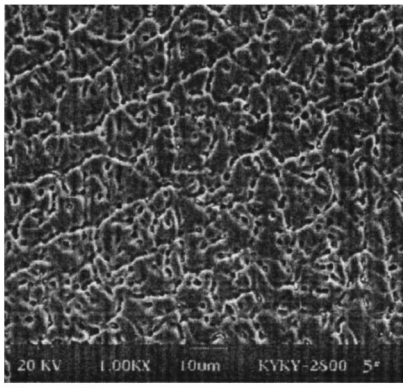

(b)

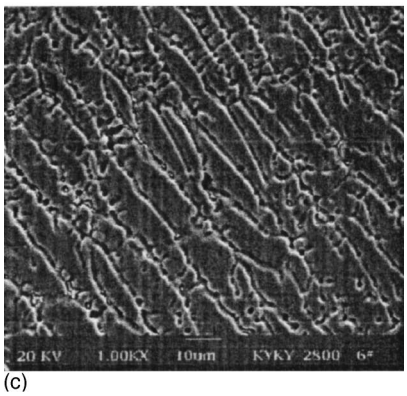

(c)

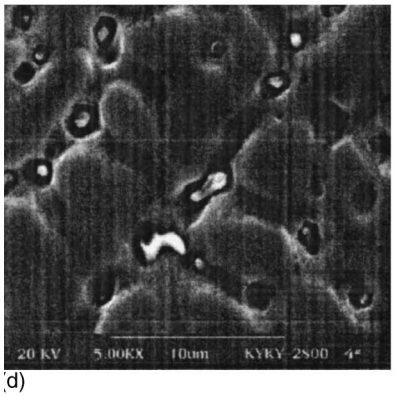

(d)

FIG. 2. Laser synthesized NiAl intermetallic layer and its microstructure: (a) basic morphology, (b) microstructure in the upper and middle zone, (c) microstructure in lower and side zone, and (d) microstructure under high amplification.

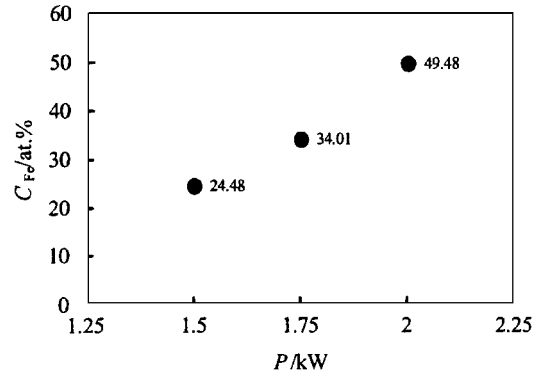

(a) laser power (D=3mm, V=7.5mm/s, Q=2.7g/min)

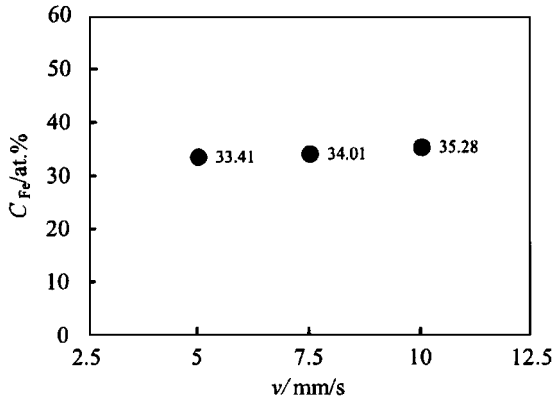

(b) scanning speed (P=1.75kW, D=3mm, Q=2.7g/min)

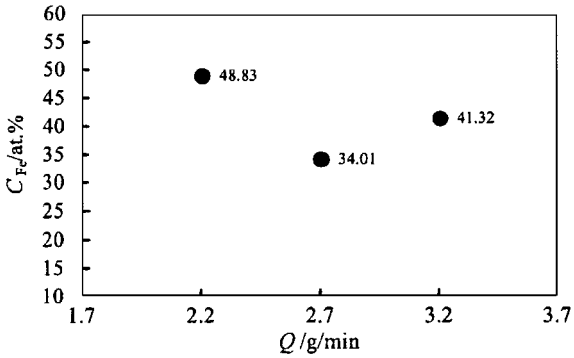

(c) powder feed rate (P=1.75kW, D=3mm, V=7.5mm/s)

FIG. 3. Relationship between the dilution rate of Fe atomic percent in the clad layer and the processing parameters.

tent. The Al lost during the laser processing ranges from 1/4 to 1/3 depending on the processing parameters.

Figure 2 shows the microstructure of the synthesized layer. The upper and middle zones in the layer contain equiaxed grain [Fig. 2(b)] while the lower and side zones contain columnar crystals [Fig. 2(c)]. This is due to the local cooling and solidification characteristics during the laser cladding process. Figure 2(d) indicates that some fine bright particles were dispersively precipitated in the grain boundary or within the grains; their composition is shown in Table I. The precipitated bright particles include mainly Ni and Fe and a few Al, which is possibly the γ phase according to its composition in the phase diagram. It is recognized that the γ

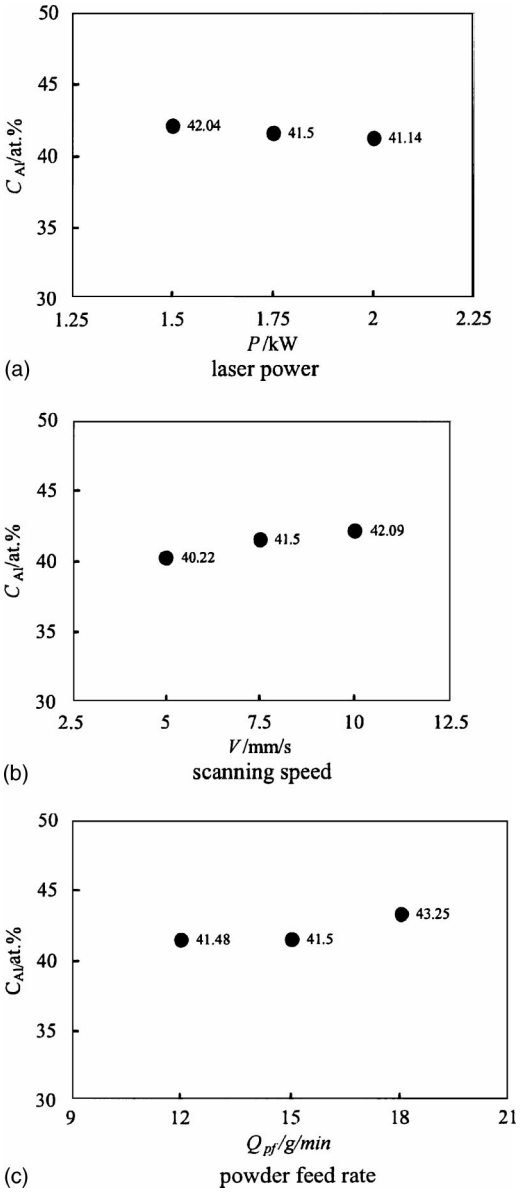

FIG. 4. Relationship between the Al content in the synthesized layer and the processing parameters.

phase may improve the toughness of the NiAl intermetallic. X-ray diffraction (XRD) analysis indicates that β-NiAl is the main phase in the synthesized layer; γ phase is not identified due to its insignificant amount (Fig. 5).

The Ni–Al phase diagram clearly indicates that NiAl intermetallic is present in the NiAl alloy in the atomic range of 41%–59% of Al. However, due to the 1/4–1/3 of Al lost in the mixed powder (Ni:Al=1:1) during the laser cladding process, the actual Ni:Al ratio in the synthesized layer is 1.2:1. Thus, there is a need to optimize the composition of

TABLE I. The composition of NiAl layer and the precipitated bright particles (at. %).

	Ni	Al	Fe
Grain	48.84	38.41	12.75
Precipitated particle	45.28	7.94	46.26

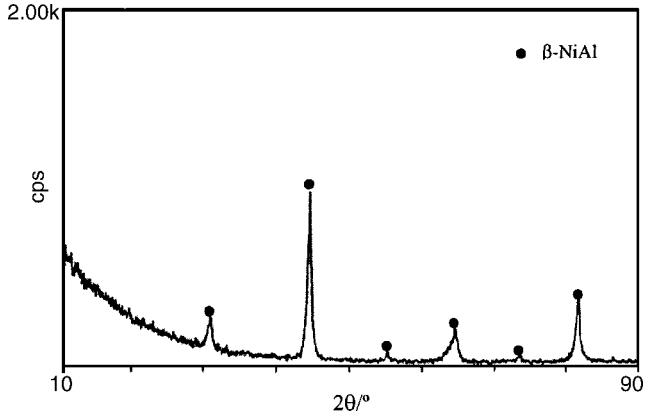

FIG. 5. X-ray diffraction result of the laser synthesized NiAl intermetallic layer.

the powder mixture and to increase the Al content in the powder mixture to balance the Al lost. An additional 1/3 pure Al powder was added to the Ni/Al clad powder to make the Ni:Al about 1:1.33. Laser synthesizing results with the same processing parameters are presented in Fig. 6. EDS analysis indicates that the deposited layer contains about 40.4 at. % of Ni, 39.6 at. % of Al, and 20 at. % of Fe (the possible C from the melted substrate was not detected). The microstructure is similar to the previous results, however, the Ni:Al ratio is 1.02:1 in the present synthesized layer. X-ray diffraction result (Fig. 7) shows stronger NiAl diffraction peaks than previous layer, implying that more NiAl synthesized in this situation.

B. Laser synthesizing TiC particulate reinforced NiAl intermetallic matrix composite

Based on the earlier research, 15–20 wt % TiC was added to the Ni/Al clad powder in order to obtain a TiC particulate reinforced NiAl IMC for better strength. The optimized processing parameters were as follows: laser power: 1.5 kW; beam diameter: 5 mm; scanning speed: 4 mm/s; and powder feed rate: 2.7 g/min. The three-layer deposition result with the same parameters is presented in Fig. 8. The synthesized layer is free of cracks; but has a few porosities. The basic microstructure of the synthesized layer can be divided into two zones: the upper zone and the lower zone. The microstructure of the laser synthesized upper zone contains some unmelted original TiC particle clusters [Fig. 9(a)], the dispersively precipitated fine TiC particles [Fig. 9(b)] and the NiAl intermetallic matrix. Figures 10(c) and 10(d) illustrate the microstructure in the lower zone, which is mainly composed of dispersively and homogeneously distributed precipitated TiC particles, the NiAl matrix, and a few unmelted original TiC particle clusters. The precipitated TiC particles are rough quadrangle and their sizes are quantitatively between micron and submicron. Figure 10 shows the interface between TiC particles and the NiAl matrix. Figure 10(a) indicates an inclusion interface between the unmelted TiC particles and the NiAl matrix. In contrast, Fig. 10(b) shows a clean interface between the precipitated TiC particle and the NiAl matrix. This implies a good interface bond between the hard phase particle and the matrix.

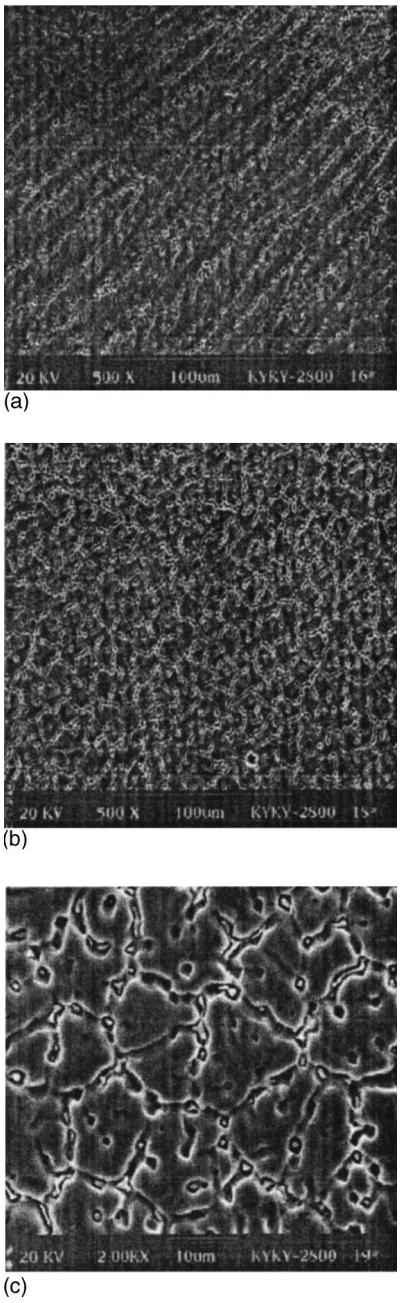

FIG. 6. Laser synthesized NiAl intermetallic layer and its microstructure for optimized powder composition: (a) microstructure in the upper and middle zone, (b) microstructure in lower and side zone, and (c) microstructure under high amplification.

Figure 11 presents an XRD result of the synthesized layer, which is identical to the standard data of β-NiAl phase and TiC phase. Therefore, the laser synthesized layers do contain β-NiAl phase and TiC phase.

Figure 12 shows the microhardness from the surface to the interface of both the synthesized NiAl layer and the TiC reinforced NiAl layer. The average microhardness is 355 $HV_{0.1}$ for NiAl, and 538 $HV_{0.1}$ for TiC reinforced NiAl. According to the energy dispersive x-ray analysis results, the real composition of the synthesized NiAl layer is: Al: 34.9%, Fe: 19.4%, and Ni: 45.6%. So the synthesized NiAl layer is in fact Ni30Al20Fe. Figure 12 indicates that TiC particulate reinforcement increases the microhardness of NiAl intermetallic alloy about 1.5 times, while maintaining its toughness as evidenced in the absence of cracks. The hardness fluctuation in the NiAl–15TiC layer was due to the three-layer deposition. The unmelted TiC particles in the upper layer and the Fe alloying effect from the melted substrate in the bottom layer increase the hardness.

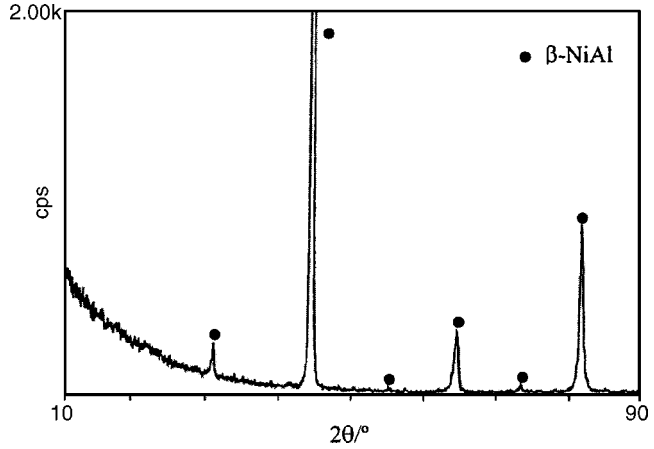

FIG. 7. X-ray diffraction result of the laser synthesized NiAl intermetallic layer with optimized powder composition.

IV. DISCUSSION

According to the binary Ni–Al phase diagram, β-NiAl phase spans a compositional range of 45%Ni–60%Ni. EDS analysis measures the actual composition to be Ni 49.2, Al 39.8, and Fe 10.9 for the NiAl layer and Ni 49.4%, Al 29.8%, Fe 19.1%, Ti 1.7% for the NiAl+TiC layer. Therefore, it is not difficult to form the β-NiAl intermetallic phase in the laser melt pool. In fact, the synthesized intermetallic should be NiAlFe. The strengthening due to the diluted Fe alloying, the rapid solidification and the fine grain size may increase the hardness of the synthesized NiAl intermetallic layer. The TiC particulate reinforcement further increases the hardness of the NiAl+TiC layer.

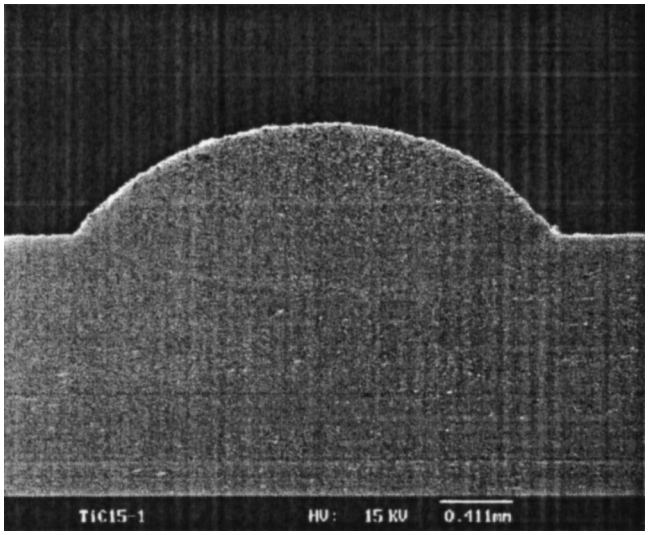

FIG. 8. Laser synthesized TiC reinforced NiAl matrix composite layer.

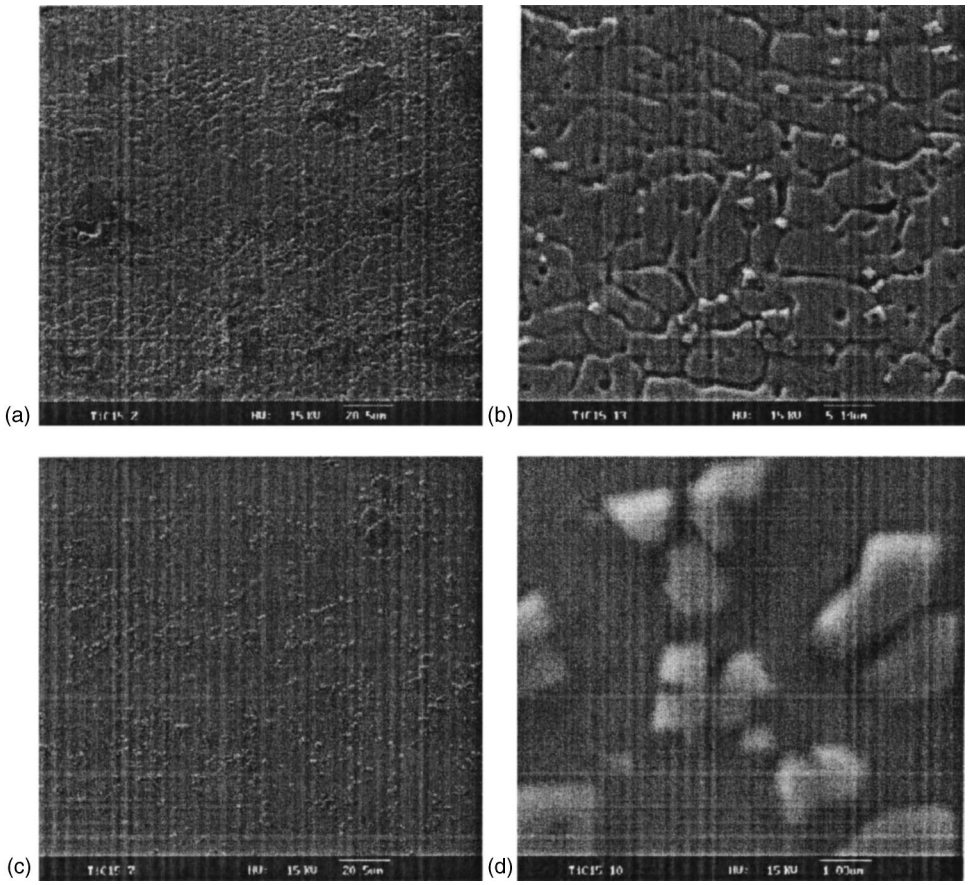

FIG. 9. NiAl intermetallic and TiC microstructure: (a) unmelted TiC particle clusters in the upper zone; (b) precipitated TiC particles in the upper zone; (c) dispersed and refined precipitated TiC particles in the lower zone; and (d) TiC particles in micron and submicron sizes in the lower region.

NiAl is a very brittle intermetallic, cracks also appear in the laser synthesized layer. However, crack-free NiAlFe layers can be achieved by optimizing laser processing parameters. Compared to the laser processing parameters which produced cracked layers, a lower laser power in combination with a slower scanning speed and larger beam diameter reduced the laser power density, slowed the heating and cooling rate and decreased the temperature gradient in laser melt pool. Thus, the thermal stress was decreased considerably. The alloying of Fe and the ductile γ phases precipitated

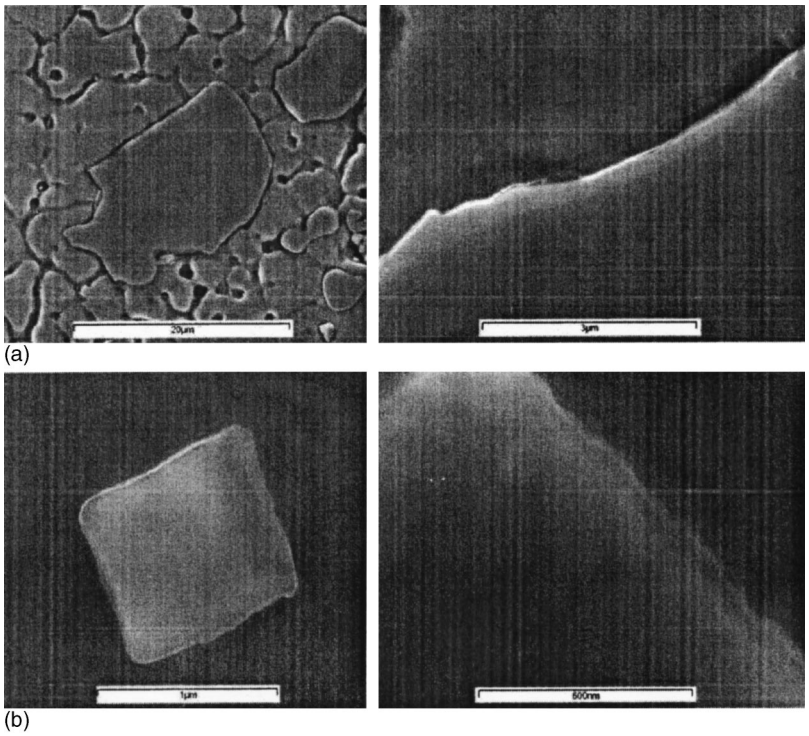

FIG. 10. Interface morphology: (a) interface between the unmelted TiC particles and the NiAl matrix; and (b) interface between the precipitated TiC particle and the NiAl matrix.

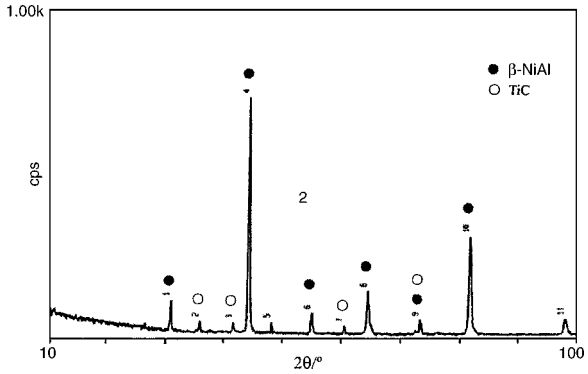

FIG. 11. X-ray diffraction result of the synthesized IMC layer.

along the crystal grain boundary may also be helpful in improving the ductility and toughness of the synthesized layers. As a result, those optimized parameters eliminated the cracks and produced fully dense NiAlFe synthesized layers.

The TiC particulate reinforcement, precipitation of ductile γ phases and crystal grain refinement may improve in the strength, ductility, and toughness of the laser synthesized layer, which may increase the properties of NiAl intermetallics. Laser synthesizing offers a promising means of producing NiAl and other intermetallics. Furthermore, it is especially significant that this method could produce not only NiAl intermetallic coating for wear, oxidation, and hot corrosion resistance at elevated temperatures, but also bulk materials or structure.

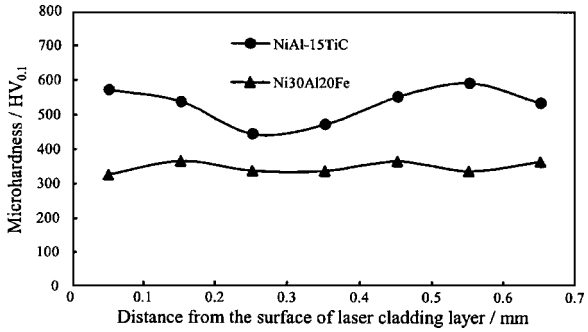

FIG. 12. Hardness distribution of the synthesized NiAl layer and TiC reinforced NiAl layer.

V. CONCLUSIONS

(1) The NiAl intermetallic and TiC particulate reinforced NiAl intermetallic matrix composite layers were successfully synthesized by laser cladding with coaxial feeding of Ni/Al clad powder and Ni/Al+TiC powder mixture respectively. With optimized processing parameters and powder mixture composition, the synthesized layers were free of cracks and metallurgical bond with the substrate.

(2) The microstructure of the laser synthesized layer was composed of β-NiAl phase and a few γ phase for NiAl intermetallic, unmelted TiC, dispersively precipitated fine TiC particles and refined β-NiAl phase matrix for TiC reinforced NiAl intermetallics composite. The microhardness was 355 $HV_{0.1}$ and 538 $HV_{0.1}$, respectively.

ACKNOWLEDGMENTS

This project was funded by the Fundamental Research Project Grant of Tsinghua University, Contract No. 985012 and the Chinese Postdoctoral Science Foundation.

[1] C. T. Liu, J. Stringer, J. N. Mundy, L. L. Horton, and P. Angelini, "Ordered intermetallics alloys: An assessment," Intermetallics **5**, 579–596 (1997).
[2] N. S. Stoloff, C. T. Liu, and S. C. Deevi, "Emerging applications of intermetallics," Intermetallics **8**, 1313–1320 (2000).
[3] G. Sauthoff, "Multiphase intermetallics alloys for structural applications," Intermetallics **8**, 1101–1109 (2000).
[4] R. Darolia, W. S. Walson, R. Noebe, A. Garg, and B. F. Oliver, "Mechanical properties of high purity single crystal NiAl," Intermetallics **7**, 1195–1202 (1999).
[5] J. E. Hack, J. M. Brzeski, and R. Darolia, "Fracture and deformation of NiAl single crystals," Mater. Sci. Eng., A **192/193**, 268–276 (1995).
[6] W. S. Walston, R. Darolia, and D. A. Demania, "Impact resistance of NiAl alloys," Mater. Sci. Eng., A **239/240**, 353–361 (1997).
[7] A. Misra and R. Gibala, "Plasticity in multiphase intermetallics," Intermetallics **8**, 1025–1034 (2000).
[8] A. Misra, R. Cibala, and R. D. Noebe, "Optimization of toughness and strength in multiphase intermetallics," Intermetallics **9**, 971–978 (2001).
[9] R. S. Chen, J. T. Guo, W. L. Zhou, and J. Y. Zhou, "Brittle to ductile transition of a multiphase intermetallic alloy based on NiAl," Intermetallics **8**, 663–667 (2000).
[10] J. D. Whittenberger, "Elevated temperature slow plastic deformation of NiAl–TiB_2 particulate composites at 1200 and 1300 K," J. Mater. Sci. **25**, 35–44 (1990).
[11] G. Jianting, Z. Lanzhang, and L. Guosong, "Research on mechanical alloying of NiAl–TiC composite," Materials Engineering **6**, 3–6 (1996) (in Chinese).